Journal of Chemical Crystallography
https://doi.org/10.1007/s10870-020-00842-5

ORIGINAL PAPER

Synthesis and Crystal Structure of Chalcone Derivatives and Their Effect on α-Glucosidase

Ping Lin[1] · Zhong-Ping Yin[1] · Meng Wang[1] · Jia Liu[1] · En Yuan[3] · Da-Yong Peng[1,2] · Xu-Liang Nie[1,2] · Xin-Chen Shang-Guan[1]

Received: 13 December 2018 / Accepted: 20 June 2020

Abstract

Five chalcone derivatives (E)-1-(2-(2-bromoethoxy)phenyl)-3-phenylprop-2-en-1-one(**1**), (E)-1-(2-(3-bromopropoxy)phenyl)-3-phenylprop-2-en-1-one(**2**),(E)-1-(2-(4-bromopropoxy)phenyl)-3-phenylprop-2-en-1-one(**3**),(E)-1-(2-(5-bromopropoxy)phenyl)-3-phenylprop-2-en-1-one(**4**),(E)-1-(2-(6-bromopropoxy)phenyl)-3-phenylprop-2-en-1-one(**5**) were synthesized and characterized by ^{1}H NMR, HRMS. The crystalline structures of compounds **4** and **5** were further characterized by X-ray crystal diffraction. Among the five compounds, **1** and **2** showed inhibitory activity on α-glucosidase, but **4** and **5** increased the activity of α-glucosidase.

Graphic Abstract

Five chalcone derivatives were synthesized and characterized by ^{1}H MNR and HRMS. The crystalline structures of two compounds were further characterized by X-ray crystal diffraction. Two of the compounds have the ability to inhibit α-glucosidase, and two different compounds have the ability to promote α-glucosidase.

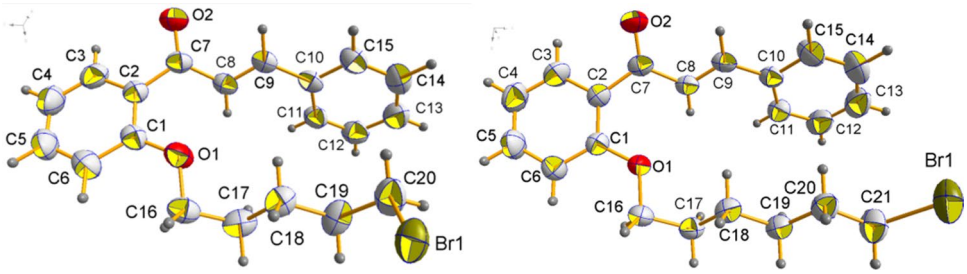

Keywords Chalcone derivatives · Synthesis · Crystal structure · α-Glucosidase

Electronic supplementary material The online version of this article (https://doi.org/10.1007/s10870-020-00842-5) contains supplementary material, which is available to authorized users.

✉ Da-Yong Peng
dayongpeng@163.com

✉ Xu-Liang Nie
13576953044@163.com

[1] Jiangxi Key Laboratory of Natural Products and Functional Foods, Jiangxi Agricultural University, Nanchang 330045, China

[2] College of Science, Jiangxi Agricultural University, Nanchang 330045, China

[3] College of Pharmacy, Jiangxi University of Traditional Chinese Medicine, Nanchang 330004, China

Introduction

Chalcones are natural organic compounds, widely found in plants, with applications in a variety of scientific domains, such as non-linear optics[1], the manufacture of dyes [2] and in supramolecular chemistry [3]. Additionally, various derivatives of chalcones have shown promise in pharmaceutical applications. Because of their privileged structures, they may display anti-diabetes [4, 5], anti-cancer [6], anti-malarial [7, 8], anti-bacterial [9, 10], anti-viral [11, 12], anti-HIV [13, 14], or anti-inflammatory activity [15]. Applications depend on the structural features, like planarity, electronic delocalization and substitution pattern on the aromatic rings

Published online: 30 June 2020

[16]. Thus, considering the potential pharmaceutical actives of the chalcone structural system, the modification of the privileged structure is an interesting goal. Toward this end, many studies have recently been carried out [17–19]. For example, chalcone derivatives were identified as potential α-glucosidase inhibitors [20].

Numerous studies reported on modifying chalcones with methoxy, hydroxyl, and nitro groups. However, very few investigations focus on chalcones with bromo side chains. An example is the crystal structure and quantum chemical investigation of chalcones with bromo butoxy side chains in the para position [21] and a report on the synthesis, characterization and crystal structure of fluoro-containing chalcone derivatives [22]. In this paper, we report the synthesis of a series of chalcones with bromo ethoxy, propoxy, butoxy, pentoxy and hexyloxy side chains in the ortho-position, as well as the crystal structures and the effects of these compounds on α-glucosidase.

Experimental

Materials and Measurements

The synthesis of 2'-hydroxychalcone was performed according to literature procedures [22]. α-Glucosidase (EC3.2.1.20) and 4-Nitrophenyl-α-D-gluocpynoaside (PNPG) were obtained from Sigma. Other reactants of AR grade were obtained commercially and used without further purification.^{1}H NMR analyses were performed on a Varian VNMR 400 MHz. The X-ray crystal structure data were collected at room temperature on a Bruker APEX II area detector diffractometer equipped with a graphite-monochromator, using Mo$K\alpha$ radiation (λ= 0.71073 Å) and ψ–ω scan mode (Scheme 1).

Synthesis of 2′-Hydroxychalcone and 1–5

Synthesis of 2′-Hydroxychalcone [22]

To a solution of equimolar amounts of 2'-hydroxyacetophenone and benzaldehyde in ethanol was added an aqueous solution of 4 M NaOH. The mixture was stirred for 2–8 h at 0 °C. The reaction mixture was neutralized with 6 M HCl and pH adjusted to 2. The mixture was then extracted with ethyl acetate, washed with water and saturated brine. It was further purified by either recrystallization or column chromatography to yield the pure compound. ^{1}H NMR (400 MHz, DMSO-d_6) δ 12.53 (s, 1H), 8.29–8.22 (m, 1H), 8.06–7.99 (m, 1H), 7.92–7.87 (m, 2H), 7.87–7.80 (m, 1H), 7.59–7.51 (m, 1H), 7.49–7.41 (m, 3H), 7.04 – 6.96 (m, 2H). ^{13}C NMR (100 MHz, DMSO-d_6) δ 193.58, 161.90,

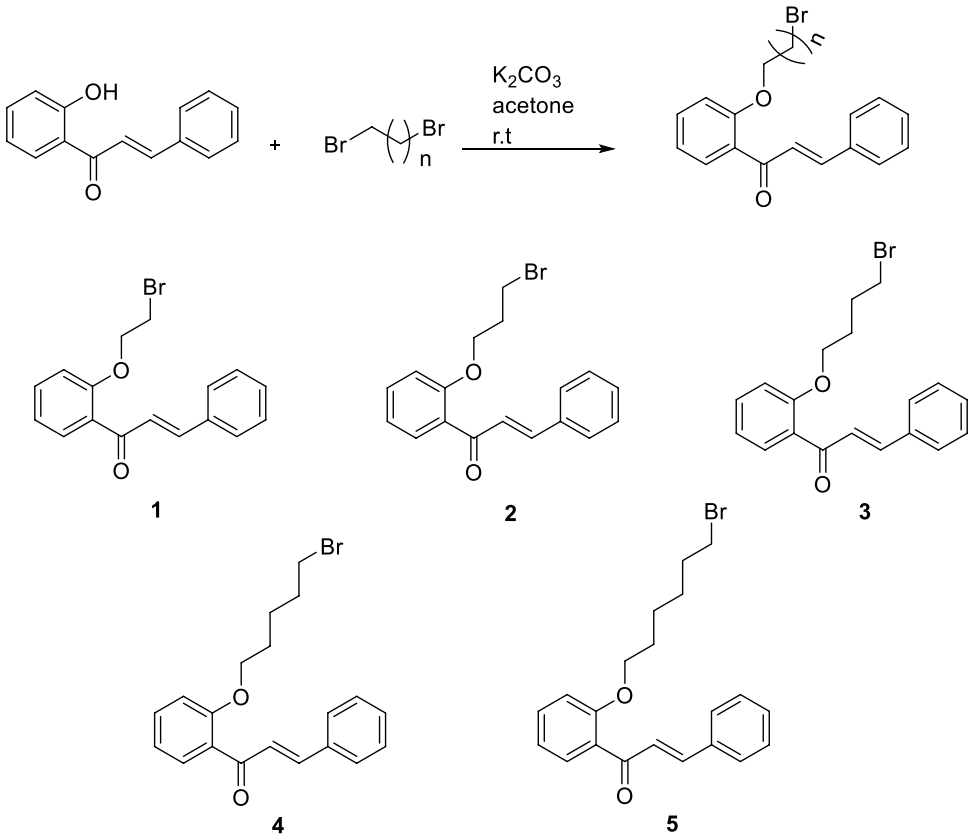

Scheme 1 Synthesis and structure of chalcone derivatives

144.74, 136.26, 134.41, 130.88, 130.83, 129.09, 128.89, 121.68, 120.68, 119.10, 117.70. HRMS (ESI) m/z: calcd for $C_{15}H_{12}O_2$ for $[M+1]^+$, calculated 225.0837, found 225.0883.

Synthesis of 1–5

1,2-Dibromoethane (8.2 g, 40.5 mmol) was added dropwise to a solution of 2′-hydroxychalcone (2 g, 13.5 mmol) and K_2CO_3(3.7 g, 27 mmol) in acetone (50 mL) at room temperature. The reaction mixture was stirred for 4–5 h. Completion of reaction was monitored by TLC analysis. After completion of the reaction, the product was extracted with ethyl acetate (3 × 50 mL) and dried with anhydrous Na_2SO_4. The product was then separated by silica gel column chromatography to obtain compound **1** as pale-yellow oil with a yield of 80%. ^{1}H NMR (500 MHz, DMSO) δ 7.79–7.74 (m, 2H), 7.63–7.59 (m, 2H), 7.59–7.56 (m, 1H), 7.55–7.52 (m, 1H), 7.46–7.40 (m, 3H), 7.19 (d, J = 8.4 Hz, 1H), 7.13–7.07 (m, 1H), 4.50–4.45 (m, 2H), 3.83–3.79 (m, 2H). ^{13}C NMR (125 MHz, DMSO) δ 191.96, 156.95, 142.69, 135.13, 133.78, 130.86, 130.51, 129.39, 129.35, 129.08, 127.43, 121.61, 113.66, 68.95, 31.73. HRMS (ESI) m/z: calcd for $C_{17}H_{15}BrO_2$ $[M + H]^+$ 330.0255, found 330.0257.

Compounds **2**, **3**, **4**, and **5** were synthesized following the procedure described for **1**. Pale yellow crystals of **4** and **5,** suitable for X-ray diffraction analysis, were obtained from ethyl acetate and acetone (V/V=1:1) with yields of 80 % and 75%, respectively.

Compound **2**: pale yellow oil; yield: 83%. ^{1}H NMR (500 MHz, DMSO) δ 7.77–7.70 (m, 2H), 7.56–7.51 (m, 3H), 7.46 (s, 1H), 7.45–7.42 (m, 3H), 7.20 (d, J=8.2 Hz, 1H), 7.11–7.05 (m, 1H), 4.20 (t, J=5.8 Hz, 2H), 3.56 (t, J=6.7 Hz, 2H), 2.29–2.19 (m, 2H). ^{13}C NMR (125 MHz, DMSO) δ 192.46, 157.30, 142.71, 134.96, 133.63, 130.95, 130.17, 129.46, 129.44, 128.92, 127.43, 121.27, 113.49, 66.46, 32.31, 31.47. HRMS (ESI) m/z: calcd for $C_{18}H_{17}BrO_2$ $[M+H]^+$ 344.0485, found 344.0482.

Compound **3**: pale yellow oil; yield: 85%. ^{1}H NMR (500 MHz, DMSO) δ 7.76–7.69 (m, 2H), 7.54 (s, 1H), 7.53–7.50 (m, 2H), 7.49 (s, 1H), 7.46–7.43 (m, 3H), 7.19 (d, J=8.1 Hz, 1H), 7.10–7.01 (m, 1H), 4.13 (t, J=6.0 Hz, 2H), 3.42 (t, J=6.5 Hz, 2H), 1.94–1.87 (m, 2H), 1.86–1.79 (m, 2H). ^{13}C NMR (125 MHz, DMSO), 157.65, 142.41, 135.06, 133.66, 130.88, 130.17, 129.45, 129.35δ 192.42, 128.89, 127.62, 121.06, 113.52, 67.73, 34.97, 29.50, 27.93. HRMS (ESI) m/z: calcd for $C_{19}H_{19}BrO_2$ $[M+H]^+$ 358.0641, found 358.0640.

Compound **4**: pale yellow crystals; yield: 80%; m.p. 58–60 ℃; ^{1}H NMR (500 MHz, DMSO) δ 7.76–7.69 (m, 2H), 7.53 (s, 1H), 7.52–7.50 (m, 2H), 7.49 (s, 1H), 7.47–7.41 (m, 3H), 7.18 (d, J=8.2 Hz, 1H), 7.09–7.03 (m, 1H), 4.10 (t, J=5.8, 2H), 3.33 (t, J=5.3 Hz, 2H), 1.76–1.65 (m, 4H), 1.50–1.41 (m, 2H). ^{13}C NMR (125 MHz, DMSO) δ 192.49, 157.79, 142.23, 135.13, 133.70, 130.85, 130.17, 129.42, 129.34, 128.84, 127.76, 121.01, 113.51, 68.42, 35.00, 32.43, 28.39, 24.89. HRMS (ESI) m/z: calcd for $C_{20}H_{21}BrO_2$ $[M+H]^+$ 372.0798, found 372.0796.

Compound **5**: pale yellow crystals; yield: 75%. m.p. 74–76 ℃. ^{1}H NMR (500 MHz, DMSO) δ 7.77–7.67 (m, 2H), 7.53 (s, 1H), 7.52–7.50 (m, 2H), 7.49 (s, 1H), 7.46–7.42 (m, 3H), 7.17 (d, J=8.1 Hz, 1H), 7.08–7.03 (m, 1H), 4.09 (t, J=6.0 Hz, 2H), 3.35 (t, J=6.8 Hz, 2H), 1.73–1.65 (m, 2H), 1.60–1.53 (m, 2H), 1.40–1.32 (m, 2H), 1.33–1.23 (m, 2H). ^{13}C NMR (125 MHz, DMSO) δ 192.46, 157.84, 142.21, 135.12, 133.71, 130.87, 130.19, 129.43, 129.31, 128.83, 127.73, 120.98, 113.46, 68.50, 35.29, 32.47, 29.11, 27.77, 25.33. HRMS (ESI) m/z: calcd for $C_{21}H_{23}BrO_2$ $[M+Na]^+$ 408.0773, found 408.0780.

Structure Determination

The crystal data for **4** and **5** were integrated using the program SAINT and corrected for absorption effects using the program SADABS [23]. The structures were solved by direct methods and refined on $F^2$by full-matrix least squares using *SHELXTL-2014* software [24]. All non-hydrogen atoms were located by direct methods and subsequent difference Fourier syntheses. The hydrogen atoms bound to carbon were placed in calculated positions and refined using a riding model. Crystallographic data and refinement information are given in Table 1.

In Vitro α-Glucosidase Inhibitory Activity Study

The inhibition activity of these compounds on α-glucosidase activity was evaluated using a micro determination model based on the reaction of α-glucosidase and 4-nitrophenyl-α-D-gluocpynoaside (PNPG). The test compounds were dissolved in DMSO and phosphate buffer (PB) to prepare the required distributing (10, 20 mmol/L) concentration. Specifically, α-glucosidase from Saccharomyces cerevisiae was assayed using a 0.01 M phosphate buffer at pH 6.8 and 10 mM PNPG as the substrate. The concentration of the enzymes was 1 U/mL in each experiment. PB (160 μL), various concentrations of the derivatives (10 μL), and α-glucosidase (10 μL) were added to 96-well polystyrene plates, and the plates were incubated at 37 °C for 20 min. After 20 min preincubation, 20 μL of PNPG solution were added to the mixture. The reaction was carried out at 37 °C for 10 min. The absorbance was measured at 405 nm using a multiscanner. Acarbose was used as the positive control in this study. The percentage of enzyme inhibition was determined by the following equation:

$$\text{Inhibition}(\%) = \left(\Delta A_{\text{control}} - \Delta A_{\text{sample}}\right)/\Delta A_{\text{control}} \times 100$$

Table 1 Crystal and structure refinement data of 4 and 5

	4	**5**
Empirical formula	$C_{20}H_{21}BrO_2$	$C_{21}H_{23}BrO_2$
CCDC deposition number	1,872,372	1,872,371
Formula weight	373.27	387.29
Temperature (K)	296(2)	296(2)
Wavelength (Å)	0.71073	0.71073
Crystal system	Triclinic	Monoclinic
Space group	P-1	$P2_1/c$
a (Å)	8.297(7)	8.3077(15)
b(Å)	8.756(8)	8.4018(15)
c(Å)	13.007(11)	26.690(5)
α(°)	90.046(11)	90
β(°)	106.892(10)	91.324(2)
γ(°)	99.507(11)	90
V(Å^3)	890.5(13)	1862.5(6)
Z	2	4
Dc (g cm-3)	1.392	1.381
Mu(MoKa) (mm)	2.315	2.217
F(000)	384	800
Crystal size (mm)	0.20×0.18×0.16	0.20×0.20×0.16
Θ range for date collection (°)	2.605–25.497	2.54–24.99
Reflections collected	6587	13,975
Independent reflection	3262 [R_{int} = 0.019]	3459 [R_{int} = 0.0181]
Goodness-of-fit on F2	1.005	1.025
Final *R* indices [$I > 2\sigma(I)$][a, b]	R_1 = 0.0779, wR_2 = 0.1895	R_1 = 0.0359, wR_2 = 0.0726
R indices (all data)[a]	R_1 = 0.1067, wR_2 = 0.2147	R_1 = 0.0545, wR_2 = 0.0803

[a] $R_1 = \Sigma \| F_o | - | F_c \| / \Sigma | F_o |$

[b] $wR_2 = [\Sigma w(F_o^2 - F_c^2)_2 / \Sigma w(F_o^2)^2]^{1/2}$

Results and Discussion

Crystal Structure of 4 and 5

X-ray diffraction analysis shows that compound **4** crystallizes in the triclinic space group *P-1*. The molecule is shown in the Fig. 1, and the observed bond lengths and angles are very similar to those reported in the literature for chalcone derivatives [24]. The dihedral angle between the phenyl groups is 71.61(18)º, which is larger than that reported in the literature for 3-cinnamoyl-4-hydroxybenzoic acid [25], because of the alkoxyl substituents in the ortho-position. The torsion angles of C3–C2–C7–O2, C3–C2–C7–C8, C2–C7–C8–C9, C7–C8–C9–C10, C2–C1–O1–C16, C1–O1–C16–C17, O1–C16–C17–C18, C16–C17–C18–C19, C17–C18–C19–C20 and C18–C19–C20–Br are 25.413(740)°, − 153.152(512)°, − 148.287(517)°, 178.107(490)°, − 167.363(462)°, 160.445(454)°, 65.284(621)°, 178.329(506)°, 179.273(548)° and 79.096(667)°, respectively.

Compound **5** crystallizes in the monoclinic space group $P2_1/c$. In the molecule of **5** (shown in the Fig. 2), bond lengths and angles are unexceptional and agree well with those reported in the literature for chalcone derivatives [26]. The dihedral angle between the phenyl groups is 56.12(9)º. The Br1–C21–C20–C19 torsion angle in structure **5** is 178.78(16)º and Br is in a *trans* position, whereas the B1–C20–C19–C18 torsion angle in structure **4** is 67.1(6)º and Br is in a gauche conformation.

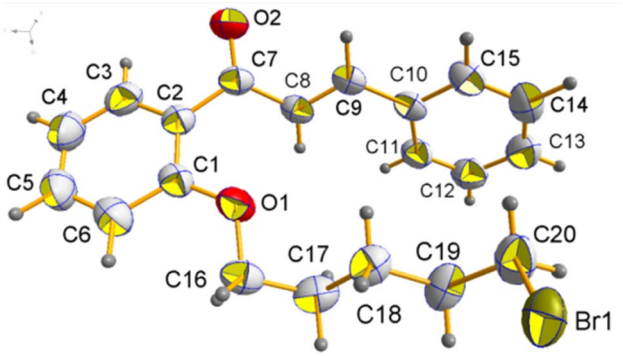

Fig. 1 Crystal structure of 4 with 30% displacement ellipsoids

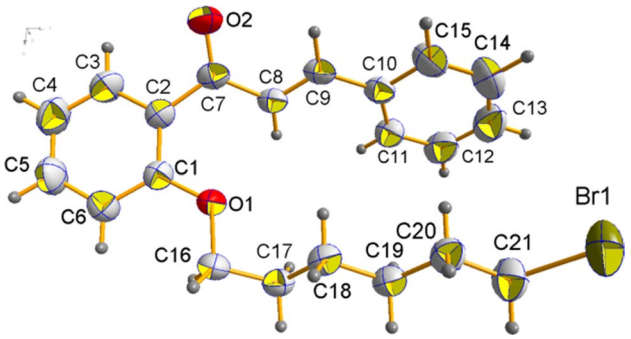

Fig. 2 Crystal structure of 5 with 30% displacement ellipsoids

We tried but failed to crystallize the oils we obtained for compound **1**, **2** and **3** using the same methods there were successful for compound **4** and **5**. Likely, the shorter side chains in are responsible for this behavior.

In Vitro α-Glucosidase Inhibitory Activity

In order to explore the synergistic biological potential of the synthesized molecules, they were subjected to in vitro α-glucosidase inhibition using the same concentrations (10 mmol/L, 20 mmol/L) for all experiments Table 2. Compounds **1**, **2** and **3** exhibited inhibition activities and may have the potential in preventing the rise of postprandial glucose levels in diabetics. Compounds **4** and **5**, however, are not inhibiting α-glucosidase. Yet, our results indicate that the length of the side chain has a large impact on α-glucosidase inhibition. The side chain length influenced the activity of α-glucosidase had been reported previously [27].The 1-deoxynojirimycin (1-DNJ) with *N*-alkyl chain of various length showed different inhibition effect [28]. Addition, a class of α-glucosidase inhibitors were synthesized based on iminofuranosides with various alkyl groups substituted at the anomeric position. These compounds showed a strong correlation between chain length and inhibition activities, neither short nor long chain length showed less activity [29]. Our results are similar with previous studies. Since all compounds showed less than 50% inhibition, we did not further evaluate them for half maximal inhibitory concentration (IC_{50}).

Supplementary Data

Supplementary data CCDC Numbers 1872371 and 1872372 contain the supplementary crystallographic data for the structures reported in this paper. Copies of this information may be obtained free of charge from the Director, CCDC, 12 Union Road, Cambridge CB2 1EZ, UK (Fax: (+44)1223 336-033; e-mail: deposit@ccdc.cam.ac.uk or https://www.ccdc.cam.ac.uk) or also available from the author Xu-Liang Nie.

Table 2 α-Glucosidase inhibition ratio at different concentrations (mmol/L)

Compd	Structure	Inhibition ratio (%)	
		10 mmol/L	20 mmol/L
1	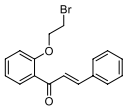	9.22	15.75
2	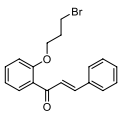	5.28	10.44
3	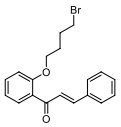	–	2.11
4	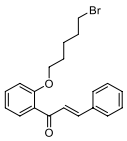	– 10.60	– 14.39
5	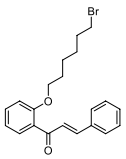	– 4.08	– 10.42
Acarbose		38.33	49.32
2′-Hydroxychalcone		2.79	5.32

Acknowledgements This work was supported by The National Natural Science Foundation of China (No. 31460436, 31260368), Scientific Research Project of Jiangxi Food and Drug Administration (No.2017sp28). The Research Foundation of Educational Department of Jiangxi Province [No. GJJ160382]. X-ray data were collected at Instrumental Analysis Center Nanchang Hang Kong University, Nanchang, 330063, People's Republic of China.

References

1. Maragatham G, Selvarani S, Rajakumar P, Lakshmi S (2018) Structure determination and quantum chemical analysis of chalcone derivatives. J Mol Struct. https://doi.org/10.1016/j.molstruc.2018.11.048
2. Teo KY, Tiong MH, Wee HY, Jasin N, Liu Z-Q, Shiu MY, Tang JY, Tsai J-K, Rahamathullah R, Khairul WM, Tay MG (2017) The influence of the push-pull effect and a π-conjugated system in conversion efficiency of bis-chalcone compounds in a dye sensitized solar cell. J Mol Struct 1143:42–48. https://doi.org/10.1016/j.molstruc.2017.04.059
3. Low JN, Cobo J, Nogueras M, Sánchez A, Albornoz A, Abonia R (2002) A comparison of the supramolecular structures of 1-(6-amino-1,3-benzodioxol-5-yl)-3-(3,4,5-trimethoxyphenyl)

prop-2-en-1-one and 1-(6-amino-1,3-benzodioxol-5-yl)-3-[4-(N, N-dimethylamino)phenyl]prop-2-en-1-one. Acta Crystallogr C 58(Pt 1):42–45. https://doi.org/10.1107/s0108270101018297
4. Bak EJ, Hong GP, Lee CH, Lee TI, Woo GH (2011) Effects of novel chalcone derivatives on α-glucosidase, dipeptidyl peptidase-4, and adipocyte differentiation in vitro. BMB Rep 44(6):410–414. https://doi.org/10.5483/BMBRep.2011.44.6.410
5. Singh P, Anand A, Kumar V (2014) Recent developments in biological activities of chalcones: a mini review. Eur J Med Chem 85(45):758–777. https://doi.org/10.1002/chin.201445285
6. Mayur YCGJP, RajendraPrasad VVS, Lemos C, Sathish NK (2009) Design of new drug molecules to be used in reversing multidrug resistance in cancer cells. Curr Cancer Drug Targets 9(3):298–306. https://doi.org/10.2174/156800909788166619
7. Chen M, Theander TG, Christensen SB, Hviid L, Zhai L, Kharazmi A (1994) Licochalcone A, a new antimalarial agent, inhibits in vitro growth of the human malaria parasite *Plasmodium falciparum* and protects mice from *P yoelii* infection. Antimicrob Agents Chemother 38(7):1470–1475. https://doi.org/10.1128/aac.38.7.1470
8. Yadav N, Dixit SK, Bhattacharya A, Mishra LC, Sharma M, Awasthi SK, Bhasin VK (2012) Antimalarial activity of newly synthesized chalcone derivatives in vitro. Chem Biol Drug Des 80(2):340–347. https://doi.org/10.1111/j.1747-0285.2012.01383.x
9. Choi D, Park JC, Lee HN, Moon JH, Ahn HW, Park K, Hong J (2018) In vitro osteogenic differentiation and antibacterial potentials of chalcone derivatives. Mol Pharm 15(8):3197–3204. https://doi.org/10.1021/acs.molpharmaceut.8b00288
10. Shakhatreh MA, Al-Smadi ML, Khabour OF, Shuaibu FA, Hussein EI, Alzoubi KH (2016) Study of the antibacterial and antifungal activities of synthetic benzyl bromides, ketones, and corresponding chalcone derivatives. Drug Des Devel Ther 10:3653–3660. https://doi.org/10.2147/dddt.S116312
11. Herencia F, Ferrándiz ML, Ubeda A, Guillén I, Dominguez JN, Charris JE, Lobo GM, Alcaraz MJ (1999) Novel anti-inflammatory chalcone derivatives inhibit the induction of nitric oxide synthase and cyclooxygenase-2 in mouse peritoneal macrophages. FEBS Lett 453(1–2):129–134. https://doi.org/10.1016/s0014-5793(99)00707-3
12. Jin YL, Jin XY, Jin F, Sohn DH, Kim HS (2008) Structure activity relationship studies of anti-inflammatory TMMC derivatives: 4-dimethylamino group on the B ring responsible for lowering the potency. Arch Pharm Res 31(9):1145–1152. https://doi.org/10.1007/s12272-001-1281-7
13. Sharma H, Patil S, Sanchez TW, Neamati N, Schinazi RF, Buolamwini JK (2011) Synthesis, biological evaluation and 3D-QSAR studies of 3-keto salicylic acid chalcones and related amides as novel HIV-1 integrase inhibitors. Bioorg Med Chem 19(6):2030–2045. https://doi.org/10.1016/j.bmc.2011.01.047
14. Uchiumi F, Hatano T, Ito H, Yoshida T, Tanuma S (2003) Transcriptional suppression of the HIV promoter by natural compounds. Antivir Res 58(1):89–98. https://doi.org/10.1016/s0166-3542(02)00186-9
15. Liu Z, Tang L, Zou P, Zhang Y, Wang Z, Fang Q, Jiang L, Chen G, Xu Z, Zhang H, Liang G (2014) Synthesis and biological evaluation of allylated and prenylated mono-carbonyl analogs of curcumin as anti-inflammatory agents. Eur J Med Chem 74:671–682. https://doi.org/10.1016/j.ejmech.2013.10.061
16. Lokesh BVS, Prasad YR, Shaik AB (2019) Synthesis, biological evaluation and molecular docking studies of new pyrazolines as an antitubercular and cytotoxic agents. Infect Disord Drug Targets 19(3):310–321. https://doi.org/10.2174/1871526519666181217120626
17. Ming LS, Jamalis J, Al-Maqtari HM, Rosli MM, Sankaranarayanan M, Chander S, Fun HK (2017) Synthesis, characterization, antifungal activities and crystal structure of thiophene-based heterocyclic chalcones. Chem Data Collect. https://doi.org/10.1016/j.cdc.2017.04.004
18. Barakat A, Al-Majid AM, Soliman SM, Islam MS, Ghawas HM, Yousuf S, Choudhary MI, Wadood A (2017) Monoalkylated barbiturate derivatives: X-ray crystal structure, theoretical studies, and biological activities. J Mol Struct 1141:624–633. https://doi.org/10.1016/j.molstruc.2017.04.017
19. de Mello MVP, Abrahim-Vieira BA, Domingos TFS, de Jesus JB, de Sousa ACC, Rodrigues CR, Souza AMT (2018) A comprehensive review of chalcone derivatives as antileishmanial agents. Eur J Med Chem 150:920–929. https://doi.org/10.1016/j.ejmech.2018.03.047
20. Sun H, Li Y, Zhang X, Lei Y, Ding W, Zhao X, Wang H, Song X, Yao Q, Zhang Y, Ma Y, Wang R, Zhu T, Yu P (2015) Synthesis, α-glucosidase inhibitory and molecular docking studies of prenylated and geranylated flavones, isoflavones and chalcones. Bioorg Med Chem Lett 25(20):4567–4571. https://doi.org/10.1016/j.bmcl.2015.08.059
21. Maragatham G, Selvarani S, Rajakumar P, Lakshmi S (2017) Crystal structures of three 1-[4-(4-bromo-but-oxy)-phen-yl] chalcone derivatives: (E)-1-[4-(4-bromo-but-oxy)-phen-yl]-3-phenyl-prop-2-en-1-one, (E)-1-[4-(4-bromo-but-oxy)-phen-yl]-3-(4-meth-oxy-phen-yl)prop-2-en-1-one and (E)-1-[4-(4-bromo-but-oxy)-phen-yl]-3-(3,4-di-meth-oxy-phen-yl)prop-2-en-1-one. Acta Crystallogr E Crystallogr Commun 73(Pt 8):1232–1236. https://doi.org/10.1107/s2056989017010052
22. Karki R, Jun KY, Kadayat TM, Shin S, Thapa Magar TB, Bist G, Shrestha A, Na Y, Kwon Y, Lee ES (2016) A new series of 2-phenol-4-aryl-6-chlorophenyl pyridine derivatives as dual topoisomerase I/II inhibitors: synthesis, biological evaluation and 3D-QSAR study. Eur J Med Chem 113:228–245. https://doi.org/10.1016/j.ejmech.2016.02.050
23. Bruker (2005) APEX2, SAINT and SADABS. Bruker AXS Inc, Madison
24. Song Z, Kwok RT, Zhao E, He Z, Hong Y, Lam JW, Liu B, Tang BZ (2014) A ratiometric fluorescent probe based on ESIPT and AIE processes for alkaline phosphatase activity assay and visualization in living cells. ACS Appl Mater Interfaces 6(19):17245–17254. https://doi.org/10.1021/am505150d
25. Chun-Mei G, Xiu-Ying S, Mi-Na W, Jia G, Xu-Liang N (2020) Crystal structure of 3-cinnamoyl-4-hydroxybenzoic acid, $C_{16}H_{12}O_4$. Zeitschrift für Kristallographie. https://doi.org/10.1515/ncrs-2020-0178
26. Sheldrick GM (2008) A short history of SHELX. Acta Crystallogr A 64(Pt 1):112–122. https://doi.org/10.1107/s0108767307043930
27. Ghani U (2015) Re-exploring promising α-glucosidase inhibitors for potential development into oral anti-diabetic drugs: finding needle in the haystack. Eur J Med Chem 103:133–162. https://doi.org/10.1016/j.ejmech.2015.08.043
28. Cendret V, Legigan T, Mingot A, Thibaudeau S, Adachi I, Forcella M, Parenti P, Bertrand J, Becq F, Norez C, Désiré J, Kato A, Blériot Y (2015) Synthetic deoxynojirimycin derivatives bearing a thiolated, fluorinated or unsaturated N-alkyl chain: identification of potent α-glucosidase and trehalase inhibitors as well as F508del-CFTR correctors. Org Biomol Chem 13(43):10734–10744. https://doi.org/10.1039/c5ob01526j
29. Natori Y, Imahori T, Murakami K, Yoshimura Y, Nakagawa S, Kato A, Adachi I, Takahata H (2011) The synthesis and biological evaluation of 1-C-alkyl-L-arabinoiminofuranoses, a novel class of α-glucosidase inhibitors. Bioorg Med Chem Lett 21(2):738–741. https://doi.org/10.1016/j.bmcl.2010.11.112